ELSEVIER

Journal of Alloys and Compounds 275–277 (1998) 258–263

Journal of ALLOYS AND COMPOUNDS

Electronic structure of Pr^{3+} and Tm^{3+} doped $LiYO_2$

Oon Kyoung Moune*, Jeannette Dexpert-Ghys, Bernard Piriou, Marie-Gabrielle Alves, Michèle D. Faucher

Laboratoire de Physico-Chimie Moléculaire et Minérale, URA 1907 du CNRS, Ecole Centrale Paris, 92295 Châtenay-Malabry Cedex, France

Abstract

An optical investigation of $LiYO_2$ doped with 2% Pr^{3+} and 5% Tm^{3+} is presented. The unit cell is monoclinic and the site symmetry at the rare earth site is C_1. The absorption, excitation and fluorescence spectra at 20 K are utilized to determine the electronic structure of the ground $4f^2$ and $4f^{12}$ configurations respectively. For $LiYO_2$:Pr^{3+}, 64 energy levels from $^3H_4$ up to $^3P_2$ at 22 000 cm^{-1} are reported. For $LiYO_2Tm^{-1}$, 58 energy levels from $^3H_6$ up to $^3P_2$ at 38 000 cm^{-1} and the relative intensities for absorption from the $^3H_6$ ground state are given. A crystal field analysis of the data is performed. Configuration interaction is applied to $LiYO_2$:Pr^{3+} and improves the results. While Eu^{3+} and Tb^{3+} doped $LiYO_2$ are good red and green phosphors respectively, $LiYO_2$:5%Tm^{3+} luminesces only weakly. The reason for that is the existence of many possible paths for up-conversion processes. © 1998 Elsevier Science S.A.

Keywords: Pr^{3+} and Tm^{3+} spectroscopy; Crystal field; $LiYO_2$; Configuration interaction

1. Introduction

At room temperature, the two structural forms stated for $LiYO_2$ activated with trivalent lanthanide ions are the tetragonal α form (space group $I4_1/amd$) isomorphous with $FeLiO_2$ [1–5] and the monoclinic β form (space group $P2_1/c$) [3,6] which arises from a deformation of the tetragonal one. We reported earlier [7] a reversible phase transition from the monoclinic to the tetragonal form in polycrystalline 5% Eu^{3+} doped $LiYO_2$ at 350 K. We reported elsewhere on the structural evolution of the $LiYO_2$:5% Ln^{3+} compounds along the rare earth series [8]. $LiYO_2$:5% Er^{3+} is monoclinic while $LiYO_2$:5% Yb^{3+} is tetragonal. Small quantities of Tb^{4+} in the Tb^{3+} doped $LiYO_2$ provoke a phase transition from the monoclinic to the tetragonal form. Recently the crystal structure of the 5% Eu^{3+} doped compound was refined by neutron diffraction techniques at room temperature and at 110°C (below and above the phase transition respectively) [9].

Only a small number of spectroscopic works have been reported on rare earth doped LiYO2 [10–14]. It was reported earlier that Eu activated LiYO2 is an efficient phosphor [15–17]. In Refs. [7,8] the energy levels and the crystal field parameters of Eu^{3+} in the monoclinic, and tetragonal forms were deduced from the fluorescence spectra at 77 K, 300 K and 370 K. In Ref. [8] the energy levels of the $4f^8$ configuration of Tb^{3+} up to 21 000 cm^{-1} were determined and the crystal field parameters of Tb^{3+} were refined. The luminescent efficiency of Eu^{3+} and Tb^{3+} doped $LiYO_2$ was compared with that of commercial standards. Ref. [18] reports on the oscillator strengths, the magnetic splitting factors, the paramagnetic susceptibility and the crystal field parameters of Nd^{3+} doped $LiYO_2$.

In order to provide more spectroscopic data from additional members of the lanthanide series and to establish trends for all the crystal field parameters in Ln^{3+} doped $LiYO_2$, we have undertaken a spectroscopic investigation of Pr^{3+} and Tm^{3+} doped compounds. The synthesis process was described earlier [8]. The praseodymium doped compound was heated at 1000°C in an $Ar+H_2$ atmosphere to reduce Pr^{4+} into Pr^{3+}. Heating $LiYO_2$ at 250°C slowly decomposes the compound into the oxides. The compound is stable at room temperature.

2. Site symmetry–spectroscopic investigation

The complementary electronic configurations of Pr^{3+} and Tm^{3+} ions ($4f^2$ and $4f^{12}$ respectively) give rise to thirteen levels: $^3H_{4,5,6}$, $^3F_{2,3,4}$, $^1G_4$, $^1D_2$, $^3P_{0,1,2}$, $^1I_6$ and $^1S_0$. At room temperature 2% Pr^{3+} and 5% Tm^{3+} doped $LiYO_2$ samples are monoclinic and the $(2J+1)$ degeneracy of the free ion levels is completely lifted by the C_1 crystal field.

*Corresponding author.

0925-8388/98/$19.00 © 1998 Elsevier Science S.A. All rights reserved.
PII: S0925-8388(98)00316-8

For both Pr^{3+} and Tm^{3+}, the whole configuration (except the $^1S_0$ range) was explored, that is, from 0 to 22 000 cm^{-1} for Pr^{3+} and from 0 up to 38 000 cm^{-1} for Tm^{3+}. The energy levels were determined by means of absorption, emission, and excitation spectra at 20 K.

The samples for the absorption experiment were in the form of a KBr pellet fastened on the cold finger of a He closed cycle cryostat (CP-62-ST/5 of Cryophysics). The concentrations were 2 and 5 mole % for the Pr^{3+} doped sample and 5 mole % for the Tm^{3+} doped sample. The spectra were recorded with a CARY 5E spectrometer in the spectral domain 430–2400 nm for the Pr^{3+} doped sample and 260–1800 nm for the Tm^{3+} doped sample.

For the fluorescence experiments coumarin 460 and rhodamine 610 pumped by the third harmonic of a Nd: YAG pulsed laser (Spectra Physics Quanta Ray DCR4) were utilized. Time-resolved fluorescence was obtained via a digital oscilloscope coupled with a microcomputer [19].

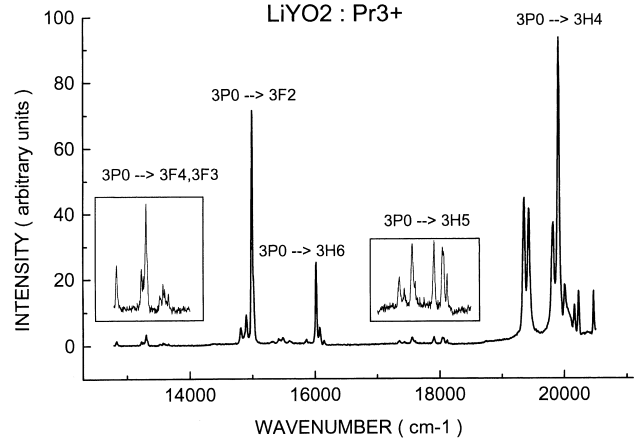

Fig. 1. The emission spectrum at 40 K of $LiYO_2$:Pr^{3+} 5% between 12 000 and 20 000 cm^{-1} obtained by excitation in the $^3P_2$ levels at 21 943 cm^{-1}.

3. Results

3.1. $LiYO_2$:Pr^{3+}

At 20 K, only the ground state is populated, therefore the absorption spectra represent directly the positions of the excited states.

The absorption spectra of a 5% Pr^{3+} doped compound revealed the presence of impurities. The main impurity was Pr_2O_3, checked by comparison with the absorption spectrum of pure Pr_2O_3. Considering the intensities of the Pr^{3+} spectral lines, the amount of Pr^{3+} in Pr_2O_3 was roughly of the same order of magnitude as the amount of Pr^{3+} in $LiYO_2$. This seems to indicate that the maximum Pr^{3+} concentration which can be really introduced into LiYO2 is much lower than 5%. In the same sample, another unidentified impurity causes spurious lines at 6365, 6382 and 6444 cm^{-1}. All the impurity lines disappear in the 2% doped compound. The results on LiYO2:Pr^{3+} discussed hereafter will refer to the 2% doped sample. 54 absorption lines corresponding to the $^3H_{5,6}$, $^3F_{2,3,4}$, $^1G_4$, $^1D_2$, $^3P_{0,1,2}$, and $^1I_6$ levels were assigned. They were confirmed by emission and excitation spectra. Fig. 1 represents the emission spectrum of $LiYO_2$:Pr^{3+} between 12 000 and 20 000 cm^{-1} obtained while exciting at 21943 cm^{-1} into a broad band of $^3P_2$ levels. The strongest emissions are that of $^3P_0 \rightarrow {}^3H_4$ and $^3P_0 \rightarrow {}^3F_2$.

A total of 64 Stark components out of the 91 levels of the $4f^2$ configuration were determined; they are listed in Table 1.

For Eu^{3+} doped $LiYO_2$, an anti-Stokes fluorescence from the $^5D_3$ level after excitation into $^5D_0$, was reported [8]. In $LiYO_2$:Pr^{3+} at 20 K, a weak anti-Stokes emission from the $^3P_0$ level (at 20463 cm^{-1}) is observed under laser excitation at 16 439 cm^{-1} which is the energy of the second Stark component of the $^1D_2$ level. The anti-Stokes emission intensity varies quadratically with the excitation power and is likely to occur via the following two-step absorption process:

Firstly a Pr^{3+} ion pumped into the $^1D_2$ level at 16 439 cm^{-1} relaxes into the lowest $^3H_6$ level (4313 cm^{-1}). It then absorbs a second photon to reach $^1I_6$. A subsequent relaxation from $^3P_1$ to $^3P_0$ takes place, and finally the emission $^3P_0 \rightarrow {}^3H_4$. There is indeed an exact coincidence between the most efficient pump energy for up-conversion (16 439 cm^{-1}) and the energy differences: $^1D_2(2) - {}^3H_4(1) = {}^1I_6(2) - {}^3H_6(1) = 16\,439$ cm^{-1}. The same occurs for Pr^{3+} in $Y_3Al_5O_{12}$ [20]. Upon exciting into the $^3P_0$ level, an exponential decay with a 2.6 μs lifetime is observed for the $^3P_0$ level whereas the $^1D_2$ decay is characterized by a rise time and a lifetime (at a long time) equal to 41 μs. In $LiYO_2$ doped with 5 mole % Pr^{3+}, the lifetime of the $^3P_0$ and $^1D_2$ when excited in $^3P_2$ are 1.4 and 4.4 μs respectively.

3.2. $LiYO_2$:Tm^{3+}

Although the first excited level of $^3H_6$ is situated at 49 cm^{-1}, the absorption spectra at 20 K display the transitions from the ground state only. The complete spectral range of the $4f^{12}$ configuration (except $^1S_0$) was explored.

The selective excitation of the lowest $^1G_4$ component at 20 824 cm^{-1} yielded the fluorescence lines emitted from this level but also from the first Stark component lying 17 cm^{-1} higher. Temperature increase caused an increase of the relative intensities of the emission lines from this excited $^1G_4$ component allowing for identification of the associated emission lines. In this way, a majority of levels pertaining to $^3H_5$, $^3F_4$ and $^3H_6$ were determined unambiguously. The transitions $^1G_4 \rightarrow {}^3H_5$ and $^3H_4 \rightarrow {}^3H_6$ occurring in the same spectral domain i.e. 12 000–12 600 cm^{-1} were

Table 1
Experimental and calculated energy levels of $LiYO_2:Pr^{3+}$ at 20 K

	Exp.	Calc. $4f^2/4f6p$	[Exp. − Calc.]	Calc. $4f^2$	[Exp. − Calc.]
$^3H_4$	0	−40	40	−5	5
	239	254	−15	258	−19
	302	304	−2	305	−3
	463	435	28	439	24
	560	551	9	529	31
	653	658	−5	656	−3
	/	974	/	959	/
	1041	1044	−3	1046	−5
	1115	1117	−2	1107	8
$^3H_5$	2305	2303	2	2300	5
	2345	2343	2	2333	12
	2395	2397	−2	2385	10
	2417	2429	−12	2413	4
	/	2541	/	2533	/
	2558	2550	8	2556	2
	/	2768	/	2778	/
	/	2811	/	2806	/
	2903	2952	−49	2941	−38
	3031	3057	−26	3040	−9
	3112	3097	15	3079	33
$^3H_6$	4313	4306	7	4309	4
	4380	4362	18	4377	3
	4439	4426	13	4424	15
	/	4447	/	4459	/
	4606	4594	12	4595	11
	/	4795	/	4754	/
	4866	4865	1	4863	3
	4927	4932	−5	4932	−5
	4974	4964	10	4942	32
	5020	5012	8	5024	−4
	5045	5067	−22	5079	−34
	5111	5132	−21	5147	−36
	5174	5185	−11	5184	−10
$^3F_2$	5442	5450	−8	5475	−33
	5469	5485	−16	5509	−40
	5562	5559	3	5547	15
	5595	5615	−20	5595	0
	5649	5661	−12	5653	−4
$^3F_3$	6803	6796	7	6807	−4
	/	6811	/	6821	/
	6833	6831	2	6834	−1
	6864	6850	14	6847	17
	6891	6889	2	6898	−7
	6923	6898	25	6912	11
	6942	6934	8	6923	19
$^3F_4$	7139	7137	2	7122	17
	7159	7175	−16	7156	3
	7184	7197	−13	7181	3
	7204	7208	−4	7225	−21
	7233	7249	−16	7255	−22
	/	7293	/	7267	/
	7631	7616	15	7617	14
	7631	7627	4	7622	9
	7631	7629	2	7637	−6
$^1G_4$	/	9749	/	9628	/
	/	9778	/	9696	/
	/	9858	/	9772	/
	9884	9875	9	9835	49
	9951	9947	4	9885	66
	/	10113	/	9921	/
	10689	10683	6	10700	−11
	10735	10733	2	10761	−26
	10735	10736	−1	10768	−33

Table 1 (Continued)

	Exp.	Calc. $4f^2/4f6p$	[Exp. − Calc.]	Calc. $4f^2$	[Exp. − Calc.]
$^1D_2$	16356	16377	−21	16354	2
	16439	16474	−35	16521	−82
	16558	16558	0	16580	−22
	17374	17343	31	17307	67
	17412	17384	28	17372	40
$^3P_0$	20463	20450	13	20453	10
$^1I_6$	20660	20692	−32	20685	−25
$^1I_6$	20752	20730	22	20729	23
$^3P_1$	20702[a]	20852	/	20855	/
$^1I_6$	/	20901	/	20888	/
$^3P_1$	20964	20971	−7	20961	3
$^1I_6$	/	21004	/	20991	/
$^3P_1$	21046	21043	3	21047	−1
$^1I_6$	21104	21095	9	21091	13
$^1I_6$	/	21255	/	21222	/
$^1I_6$	/	21320	/	21303	/
$^1I_6$	21771	21779	−8	21787	−16
$^3P_2$	21872	21867	5	21876	−4
	/	21893	/	21915	/
	21970	21971	−1	21956	14
	21993	21991	2	22010	−17
	22031	22038	−7	22041	−10
$^1I_6$	/	22239	/	22176	/
	/	22286	/	22201	/
	/	22396	/	22335	/
	/	22501	/	22368	/
	/	22531	/	22439	/
$^1S_0$	/	47667	/	47120	/

assigned by time-resolved fluorescence. The lifetimes of $^1G_4$ and $^3H_4$ are 10.9 and 144 μs respectively. Excitation spectra monitored on the $^1G_4 \rightarrow {}^3H_6$ transition at 20 590 cm^{-1} confirmed eight $^1G_4$ Stark components obtained from the absorption spectra. Nonselective excitation with the third harmonic of the Nd:YAG laser at 355 nm confirmed the first two Stark components of $^1D_2$ and eight Stark components of $^3F_4$ determined by absorption. 5 lines at 21 570, 21 291, 21 974, 22 016, and 22 064 cm^{-1} with a very short lifetime (≈0.5 μs) could not be identified and were assigned to impurities. The 58 energy levels observed by absorption, excitation or emission are listed in Table 2.

4. Crystal field analysis

In $LiYO_2$, the coordination polyhedron around the yttrium ion is a distorted octahedron generating a C_1 site symmetry [6] which involves 27 crystal field parameters (CFP). However, due to the fact that the symmetry is not too far from cubic, there exist possibilities for some of the CFP to be small. Indeed the values predicted by the covalo-electrostatic model [21] for Eu^{3+} and Nd^{3+} doped $LiYO_2$ permitted us to keep only 11 and 9 CFP respectively [8,18]. The crystal field analysis was performed by means of program *fn* [22]. It takes into account the

Table 2
Experimental calculated energy levels of $LiYO_2:Tm^{3+}$ at 20 K. Relative intensities within J levels

	Exp.	Calc.	[Exp.−Calc.]	Irel (Exp.)
$^3H_6$	0	−12	12	/
	49	50	−1	/
	117	104	13	/
	133	135	−2	/
	209	203	6	/
	209	209	0	/
	236	245	−9	/
	/	435	/	/
	/	570	/	/
	647	669	−22	/
	/	704	/	/
	/	772	/	/
	/	804	/	/
$^3F_4$	5578	5576	2	75
	5592	5581	11	100
	5612	5602	10	45
	5956	5961	−5	50
	5992	6002	−10	30
	6082	6070	12	90
	6093	6094	−1	/
	/	6123	/	/
	6198	6216	−18	25
$^3H_5$	8255	8255	0	20
	8280	8267	13	35
	/	8312	/	/
	8349	8340	9	80
	8368	8365	3	80
	8473[a]	8565	/	45
	8586	8576	10	100
	/	8648	/	/
	8725	8761	−36	65
	/	8821	/	/
	/	8856	/	/
$^3H_4$	12565	12560	5	15
	12597	12586	11	100
	12622	12592	30	50
	12741	12749	−8	20
	12759	12769	−10	15
	12853	12852	1	10
	12910	12924	−14	35
	/	12968	/	/
	/	13158	/	/
$^3F_3$	14543	14520	23	20
	14590	14589	1	30
	14590	14599	9	/
	14600	14612	−12	5
	14615	14622	−7	100
	14701[a]	14672	/	30
	14802[a]	14681	/	5
$^3F_2$	15040	15011	29	10
	15080	15111	−31	35
	15283	15265	18	100
	15310	15301	9	50
	15343	15368	−25	15

Table 2 (Continued)

	Exp.	Calc.	[Exp.−Calc.]	Irel (Exp.)
$^1G_4$	20824	20852	−28	100
	20841	20853	−12	90
	20877	20912	−35	50
	/	21435	/	/
	21506	21493	13	40
	21558	21549	9	20
	21616	21608	8	15
	21666	21654	12	15
	21771	21743	28	15
$^1D_2$	27724	27737	−13	15
$+\,^3P_2$	27754	27760	−6	15
	27821	27822	1	10
	27864	27845	19	100
	/	27933	/	/
$^1I_6$	33745	33765	−20	25
	/	33779	/	/
	/	34012	/	/
	34056	34036	20	100
	34135	34137	−2	25
	/	34223	/	/
	/	34503	/	/
$^1I_6$	/	34564	/	/
	/	34691	/	/
	/	34766	/	/
	/	34844	/	/
	/	34941	/	/
	34964	34963	1	80
$^3P_0$	/	35026	/	/
$^3P_1$	/	35907	/	/
	35939	35946	−7	15
	36059	36052	7	100
$^3P_2$	37577	37573	4	95
$+1D_2$	/	37709	/	/
	38014	38005	9	25
	38065	38077	−12	100
	/	38203	/	/
$^1S_0$	/	73577	/	/

electronic interactions within f^n configurations, included in the following familiar expansion where the operators and parameters have their usual meaning [23].

$$H = \sum_k F^k(\mathrm{ff}) f^k + \zeta(f) A_{\mathrm{so}} + \alpha L(L+1) + \beta G(G_2) + \gamma G(R_7) + \sum_i T^i t_i + \sum_h M^h m_h + \sum_f P^f p_f + \sum_{kq} B_q^k \cdot C_q^k$$

The CFP of Eu^{3+} were utilized as starting values for Pr^{3+} and Tm^{3+}. All free-ion parameters were varied freely except γ which was kept constant and M^2, M^4, P^4 and P^6 which were constrained by the ratios $M^2 = 0.56M^0$; $M^4 = 0.38M^0$; $P^4 = 0.75P^2$; $P^6 = 0.5P^2$. Therefore, for the conventional crystal field analysis, 9 free-ion parameters and 11 CFP were fitted for Pr^{3+} and Tm^{3+}. The experimental and fitted energy levels are reported in Tables 1 and 2 for Pr^{3+} and Tm^{3+} respectively, the free ion and crystal field parameters in Table 3, along with the crystal field parameters of other members in the series. The mean deviations are equal to 23.9 and 15 cm^{-1}, and the r.m.s. deviations to 28.9 cm^{-1} and 18.6 cm^{-1} for Pr^{3+} and Tm^{3+} respectively. It is not understood why M^0 tends towards a negative value. This has already been observed in a previous work on Tm^{3+} in $LiYF_4$ [24].

Table 3
Free ion and crystal field parameters Pr^{3+} and Tm^{3+} (this work), Nd^{3+} [18], Eu^{3+} and Tb^{3+} [8] in $LiYO_2$. For Pr^{3+}, columns 2 and 3 correspond to a crystal field analysis without with configuration interaction respectively. T is the temperature, n and n_p the number and levels of parameters respectively. X^2 and X^4 are the multipliers of the theoretical values of the interconfiguration parameters ($<fp|r^2/r^3|fp>=11576$; $<fp|r^2/r^3|pf>=3249$; $<fp|r^4/r^5|pf>=2973$; $<ff|r^2/r^3|fp>=-4886$; $<ff|r^4/r^5|fp>=-2968$). All values in cm^{-1}.

	Pr^{3+} $4f^2$	Pr^{3+} $4f^2/4f6p$	Nd^{3+} $4f^3$	Eu^{3+} $4f^6$	Tb^{3+} $4f^8$	Tm^{3+} $4f^{12}$
T(K)	20	20	20	77	20	20
F^0(ff)	12399	12723				17683
F^2(ff)	66902	66911	70086			99737
F^4(ff)	50610	51611	52316			69925
F^6(ff)	33927	35102	37044			50519
α	25.0	20.7	23.5			10.3
β	−812	−739	−736			−623
γ	(1070)	(1070)	1130			(1820)
M^0	−0.80	0.66	1.65			0.79
P^2	848	654	278			207
ζ(f)	708.4	720.1	866.0			2615.7
B^2_0(ff)	−242	51	−245	−236	−185	−365
B^2_1(ff)	234	284	270	160	229	111
S^2_1(ff)	−309	−245	/	−215	/	−86
B^2_2(ff)	−35	−72	80	−93	83	−88
B^4_0(ff)	2818	3614	2623	2323	2341	2026
B^4_1(ff)	379	51	−734	16	−498	164
S^4_1(ff)	797	251	−539	−372	−360	−547
B^4_4(ff)	2046	2032	1891	1520	1613	1348
B^6_0(ff)	695	897	697	633	413	430
B^6_4(ff)	−685	−738	−548	−629	−363	−390
S^6_4(ff)	12	−443	/	64	/	−350
X^2		2.654				
X^4		3.850				
ζ(p)		(3800)				
B^2_0(fp)		−1131				
B^4_0(fp)		20693				
F_0(fp))$-F^0$(ff)		(124000)				
δ[a]	23.9	15.7	15.8	7.3	7.4	15.0
r.m.s.[b]	28.9	19.9	17.9	9.4	9.6	18.6
n	64	64	105	43	40	58
n_p	20	24	24	16	16	20

[a] $(\Sigma_{i=1,n}(Ei_{exp}-Ei_{calc})^2/n)^{1/2}$
[b] $(\Sigma_{i=1,n}(Ei_{exp}-Ei_{calc})^2/(n-n_p))^{1/2}$.

In addition to the conventional one-electron crystal field analysis within $4f^2$, a crystal field analysis involving interaction with the excited 4f6p configuration was performed for the Pr^{3+} compound. As additional parameters, it should include: 5 intra-configurational free-ion parameters $<fp|r^k/r^{k+1}|fp>(k=2)$, $<fp|r^k/r^{k+1}|pf>(k=2$ and 4), and $<ff|r^k/r^{k+1}|fp>(k=2$ and 4). Theoretical values of these parameters were evaluated numerically and only the multipliers X^k for ranks $k=2$ and 4 were varied. Theoretical Hartree–Fock values of ζ(p) and of the gap F^0(fp))$-F^0$(ff) were utilized [25]. No CFP (pp) was introduced and only B^2_0(fp) and B^4_0(fp) were involved in the fitting.

The final number of parameters amounted to 24. The fitted levels and corresponding parameters are listed in Tables 1–3. What can be noted is the decrease of the root-mean square deviation of the experimental/calculated fit from 28.9 to 19.9 cm^{-1} (31%) when configuration interaction is introduced. Such a decrease has already been stated for other Pr^{3+} compounds [26,27]. As expected, the Slater parameters F^k(ff) and the spin–orbit coupling constant ζ(f) increase with the number of f electrons (N). For the large CFP (B^4_0(ff), B^4_4(ff), B^6_0(ff) and B^6_4(ff)) a distinct decrease is observed with the increase of N. Besides, the variations of the other CFP's especially those expressing the lowering of the site symmetry from D_{2d} to C_1 are not smooth. The mean deviations (δ) do not vary smoothly either along the rare earth series but this can be explained in the following way: the $4f^3$ calculation for Nd^{3+} was performed utilizing a modified U^4 table which corrects completely the discrepant $^2H(2)_{11/2}$ level for any compound [28]. This correction has nearly the same effect as the interaction with the excited $4f^26p$ configuration [29]. Then it follows that the mean deviation for Nd^{3+} in $4f^3$ (with a modified table) is similar to the mean deviation for Pr^{3+} (with configuration interaction). Utilizing the ''normal'' U4 table causes δ to climb up to 28.4 cm^{-1}, which is similar to the δ of the plain $4f^2$ calculation for Pr^{3+}. The

case of Eu^{3+} is different: the number of levels is lower and besides, the calculated barycenters of the $J=0$–6 levels have been individually adjusted to the experimental values, a procedure which, off course, contributes to the lowering of δ. At last, it is to be noted that the mean deviations for Pr^{3+} and Tm^{3+} are approximately in the same ratio as the magnitude of the crystal field for these two ions.

References

[1] R. Hoppe, Angew. Chem. 71 (1959) 457.
[2] R. Hoppe, H.J. Röhrborn, Naturwissenschaften 48 (1961) 452.
[3] F. Bertaut, M. Gondrand, C.R. Acad. Sc. 255 (1962) 1135.
[4] H. Glaum, S. Voigt, R. Hoppe, Z. Anorg. Allg. Chem. 598–599 (1991) 129.
[5] R. Hoppe, H. Sabrowsky, Z. Anorg. Allg. Chem. 357 (1968) 202.
[6] F. Stewner, R. Hoppe, Z. Anorg. Allg. Chem. 380 (1971) 250.
[7] M. Faucher, O.K. Moune, L. Albert, B. Piriou, C.R. Acad. Sci. Paris II-317 (1993) 1569.
[8] M.D. Faucher, O.K. Moune, M.-G. Alves, B. Piriou, Ph. Sciau, M. Pham-Thi, J. Solid State Chem. 121 (1996) 457.
[9] M.D. Faucher, Ph. Sciau, J-M. Kiat, M-G Alves, F. Bourée, to be published in J. Solid State Chem.
[10] M. Blanchard, C. Linarès, F. Gaume-Mahn, C.R. Acad. Sci. Paris 271B (1970) 523.
[11] F. Gaume-Mahn, C. Linarès, M. Blanchard, Proc. 9th Rare Earth Res. Conf., vol. 2, 1971, p. 478.
[12] V.A. Antonov, P.A. Arsenev, Phys. Stat. Sol. a 32 (1975) K71.
[13] V.A. Antonov, P.A. Arsenev, S.A. Vakhidov, E.M. Ibragimova, D.S. Petrova, Phys. Stat. Sol. a 41 (1977) 45.
[14] V.A. Antonov, P.A. Arsenev, Z.A. Artykov, D.S. Petrova, Phys. Stat. Sol. a 41 (1977) 45.
[15] G. Blasse, A. Bril, J. Chem. Phys. 45 (1966) 3327.
[16] L.H. Brixner, J. Electrochem. Soc.: Solid State Science 114 (1967) 252.
[17] P.M. Jaffe, J.D. Konitzer, J. Electrochem. Soc. 116 (1969) 633.
[18] O.K. Moune, N. Edelstein, B. Piriou, M.-G. Alves, M.D. Faucher, J. Alloys Compd. 250 (1997) 310.
[19] B. Piriou, H. Rager, H. Schneider, J. Eur. Ceram. Soc. 16 (1996) 195.
[20] O.L. Malta, E. Antic-Fidancev, M. Lemaitre-Blaise, J. Dexpert-Ghys, B. Piriou, Chem. Phys. Lett. 129 (1986) 557.
[21] D. Garcia, M. Faucher, J. Chem. Phys. 82 (1985) 5554.
[22] M.D. Faucher unpublished program *fn*.
[23] W.T. Carnall, G.L. Goodman, K. Rajnak, R.S. Rana, A systematic analysis of the spectra of the lanthanides doped into single crystal LaF_3, Unpublished Report ANL-88-8 (1988).
[24] H.P. Jenssen, A. Linz, R.P. Leavitt, C.A. Morrison, D.E. Wortman, Phys. Rev. B 11 (1975) 92.
[25] R.D. Cowan, Computer program RCN31 (September 1981).
[26] M.D. Faucher, O.K. Moune, Phys. Rev. A 55 (1997) 4150.
[27] M. Faucher, H.J. Kooy, Solid State Comm. 102 (1997) 663.
[28] M. Faucher, D. Garcia, P. Porcher, C.R. Acad. Sci. Paris II-308 (1989) 603.
[29] M. Faucher, O.K. Moune, J. Alloys Compd. 250 (1997) 306.